Zovein A, Luque A 2009

1. Inventory of Supplemental Information

Please provide an inventory of all supplemental items with a short explanation of their relationship to the main figures and tables (see more detailed information above). This inventory will help the editor and reviewers to assess the Supplemental Information.

Figure S1: Provides supporting evidence to Figure 1 regarding the transgenic constructs used, β3 integrin upregulation, and the FACS analysis of embryonic cells.

Figure S2: Provides additional data to complement Figure 2, detailing luminal occlusion in other organs, and demonstrating the phenotype to be a strict endothelial phenomenon.

Figure S3: Demonstrates detailed immunohistochemical data and RNA analysis that supports and broadens the conclusions set forth in Figure 3.

Figure S4: Provides supporting evidence to Figure 4 regarding how retinal endothelial cells were evaluated, and also additional embryonic data that supports the retinal phenotype.

Figure S5: Expands upon the antibody blockade in Figure 5 by demonstrating different combinations of the antibodies used, and the detrimental effect of β3 integrin inactivation.

Figure S6: Provides the background data to Figure 6, which establishes the validity of the tagged viral construct used and the appropriate controls.

Supplemental Figures

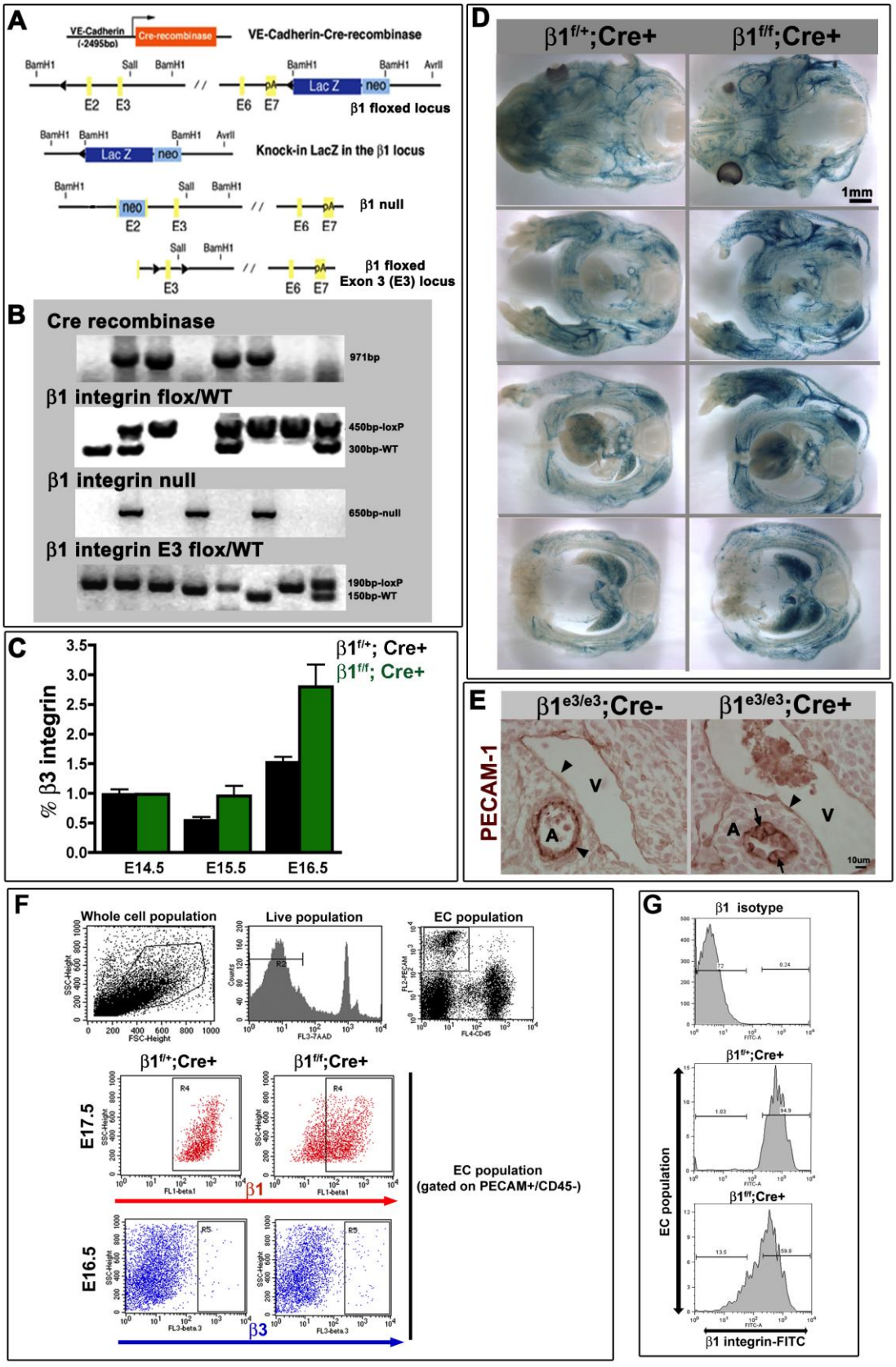

Figure S1: β1 integrin floxed constructs, efficiency of genetic deletion and compensation by β3 integrin. (A) From top to bottom: constructs of the VE-cadherin Cre recombinase transgene, "floxed" β1 integrin locus - encompasses exons 2 through 7 (20 kb) and allows expression of LacZ after Cre mediated excision (Brakebusch et al., 2000; Potocnik et al., 2000), the null allele shows disruption of the Itgb1 gene ATG site in exon 2 (Fassler and Meyer, 1995), and a floxed exon 3 allele (Raghavan et al., 2000). (B) Genotyping of tail DNA demonstrates presence of Cre recombinase (971bp), floxed (450bp) or wild-type (300bp) bands of the larger construct, as well as the null allele (650bp) and the floxed (190bp) or wild-type (150bp) bands of the smaller (E3) construct. (C) FACS analysis demonstrates an increase in the percentage of endothelial cells expressing β3 integrin protein within the $\beta1^{f/f}$; VE-cadherin Cre+ (green) group. Data shown as mean +/- SEM. (D) Vibratome sections of E14.5 embryos demonstrate extent of endothelial recombination at the β1 integrin locus (β-gal staining in blue) for homozygous and heterozygous floxed animals. (E) PECAM-1 (brown) staining of E12.5 $\beta1^{e3/e3}$; Cre+ and $\beta1^{e3/e3}$; Cre- embryos demonstrate cuboidal endothelial cell shape in arteries (A, arrows) of the homozygous floxed E3 ablated embryo, as compared to the vein (V) or littermate vessels with normal EC morphology (arrowheads). (D, E) Scale bar of each section applies to all panels. (F) Embryonic cell suspensions were gated on size, viability (7AAD), and PECAM-1+/CD45- gates (top row). Endothelial cells were then evaluated for β1 (red) and β3 (blue) integrin expression (lower rows). (G) For fluorescent cell sorting, endothelial cells (PECAM-1+/CD45-) of $\beta1^{f/f}$; Cre+ embryos (at E16.5) were further sub-grouped into populations with and without β1 integrin protein expression. Isotype and heterozygous controls also depicted.

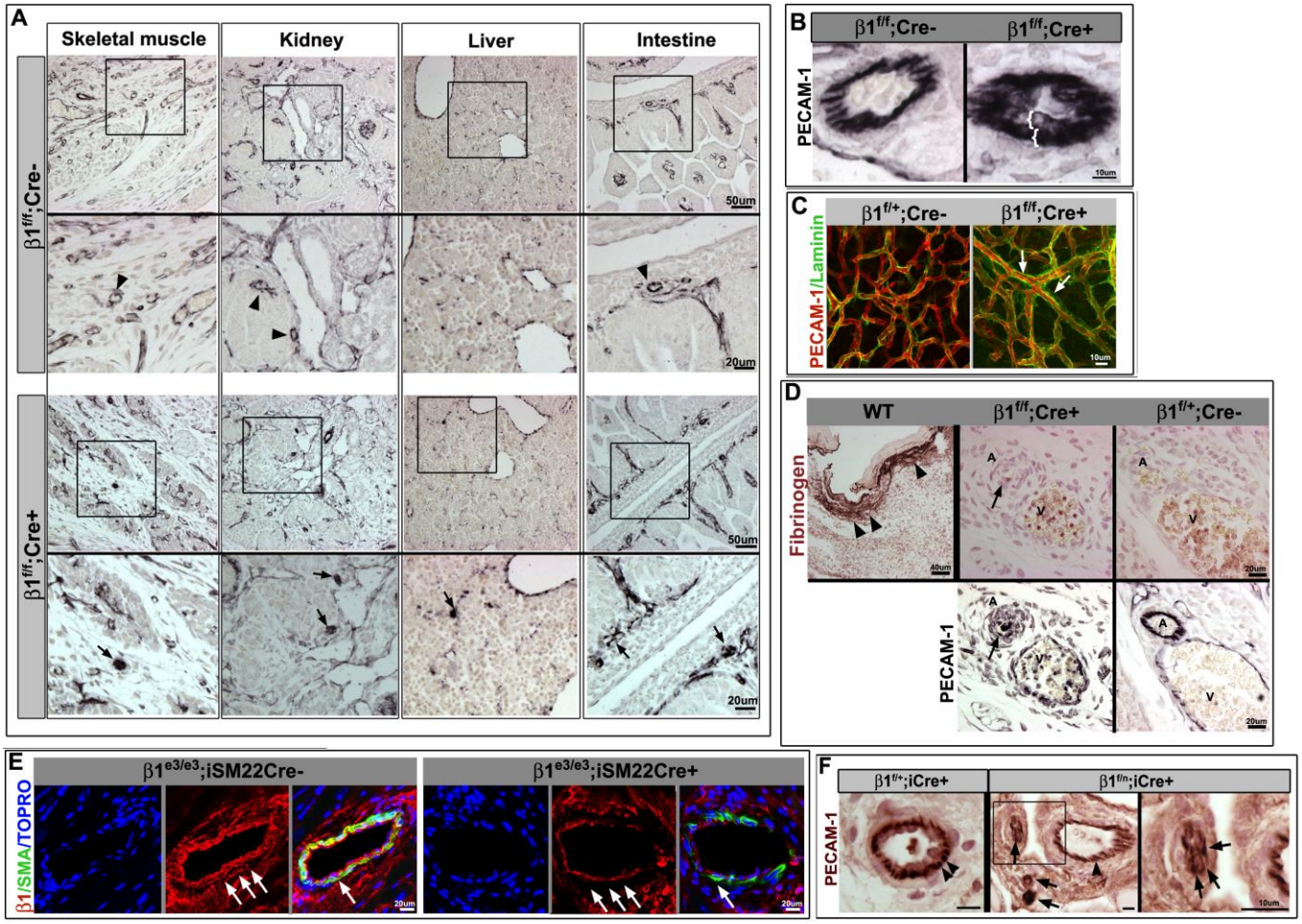

Figure S2: Luminal occlusion and stratification in endothelium upon β1 integrin loss. (A) When β1 ablated embryonic organs are evaluated (organs as labeled), multiple sites of luminal occlusion are noted (arrows) as compared to wild-type littermates (arrowheads). Lower panels are higher magnification of boxed areas. (B) Mis-localized PECAM-1 expression in arteries lacking β1 integrin also outlines the stratification (brackets) of normally single layered endothelium. (C) Abnormal laminin expression (arrows) is noted in the skin vasculature of E15.5 embryos deleted for β1 integrin. Laminin in green, PECAM-1 in red. (D) As a positive control, fibrinogen (brown) is shown within a placental clot of a wild-type adult (WT, arrowheads), but is absent in an occluded E15.5 $\beta1^{f/f}$; Cre+ artery (arrow). PECAM-1 (black) in a serial section better demonstrates the vessels and arterial occlusion (arrow). (E) β1 (red) deletion in the smooth muscle cell (SMC) compartment using an

inducible SM22 Cre line (arrows) results in abnormal SMC morphology and decreased coverage, but does not result in luminal occlusion. (F) Postnatal endothelial β1 integrin deletion (from P4-P8, evaluated at P10) using an inducible VE-cadherin Cre line ($\beta1^{f/n}$; iCre+) shows abnormal PECAM-1 (brown) expression and luminal occlusion in some arteries (arrows), but not in all vessels. Some of the larger arteries have lateral PECAM-1 distribution (arrowhead), much like induced heterozygous littermates (arrowheads). For $\beta1^{f/n}$; iCre+ : panel on right is higher magnification of boxed area on left. (A-F) Scale bars as labeled per row/section.

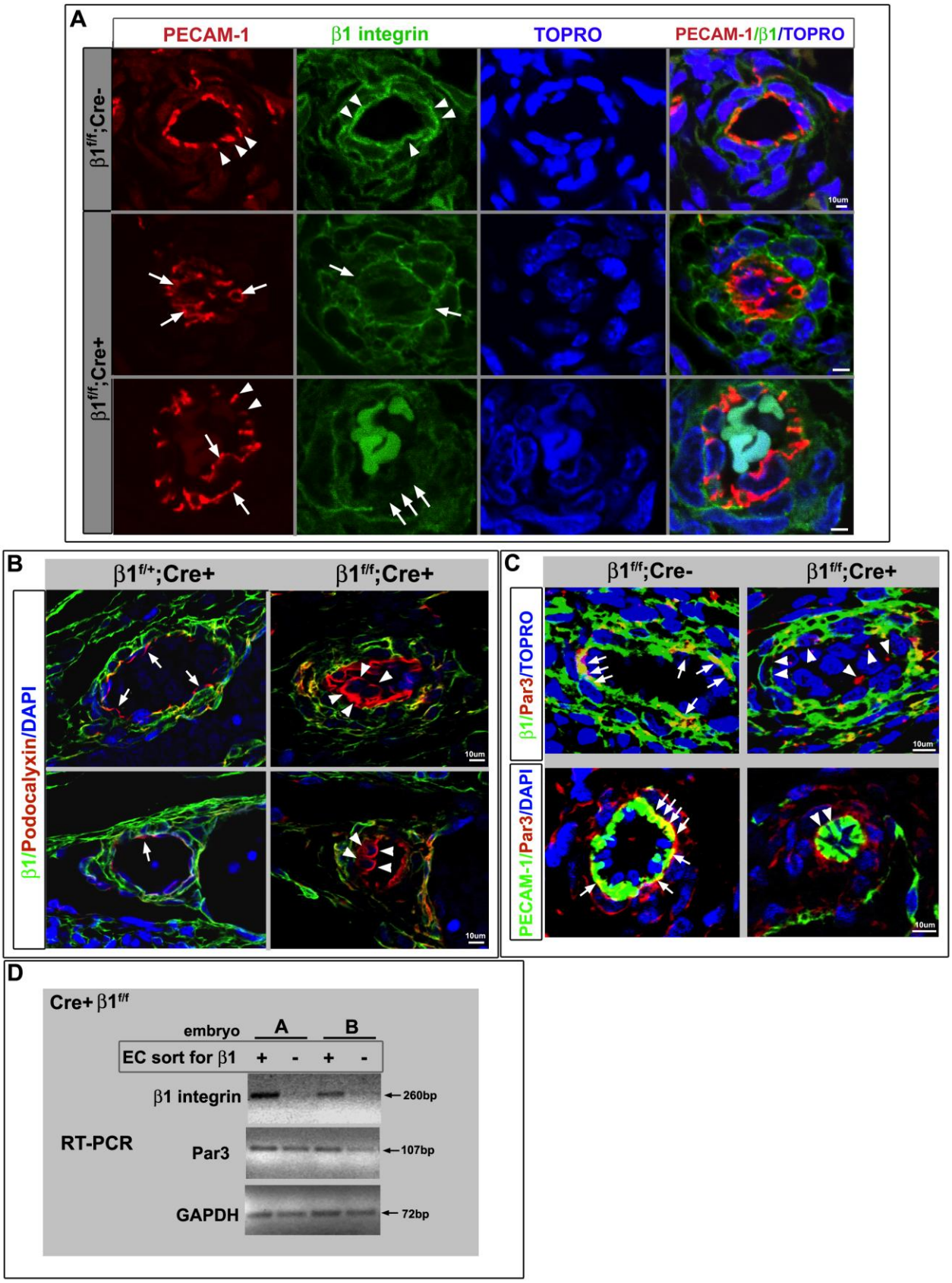
A
PECAM-1
β1 integrin
TOPRO
PECAM-1/β1/TOPRO
β1f/f;Cre-
β1f/f;Cre+
10um
B
β1f/+;Cre+
β1f/f;Cre+
β1/Podocalyxin/DAPI
10um
C
β1f/f;Cre-
β1f/f;Cre+
β1/Par3/TOPRO
PECAM-1/Par3/DAPI
10um
D
Cre+ β1f/f
embryo
A
B
EC sort for β1 + - + -
β1 integrin
260bp
RT-PCR
Par3
107bp
GAPDH
72bp

Figure S3: Changes in polarity due to β1 integrin loss. (A) E15.5 WT vessels display lateral PECAM-1 expression (red) in between squamous ECs (arrowheads). In contrast, β1 integrin (green) ablated ECs, lack this protein, and exhibit mis-localization of PECAM-1 with luminal occlusion (middle panel, arrows). In the bottom panel, a hybrid vessel shows a single EC with β1 integrin protein loss. This cell shows redistribution of PECAM-1 from lateral to apical-basal location, and abnormal shape (arrows). (B) Embryonic vessels at E15.5 demonstrate redistribution of apically located podocalyxin (red, arrows) to circumscribe endothelial cells, which have lost β1 integrin (green, arrowheads). (C) Early and late consequences of β1 integrin loss are demonstrated as the top panel depicts at E15.5 Par3 (red) and β1 integrin (green) basal co-localization in the wild-type animal (yellow, arrows) with decreased Par3 expression and abnormal localization in the $\beta1^{f/f}$; Cre+ animal (arrowheads). The bottom panel depicts a similar basal location of Par3 (red) with PECAM-1 (green) in the E17.5 wild-type (yellow, arrows), with complete loss of Par3 endothelial expression in the occluded $\beta1^{f/f}$; Cre+ vessel at E17.5 (arrowheads). (A-C) Scale bars as labeled per row/section. (D) β1 ablated endothelial cells were sorted according to β1 integrin protein expression, and mRNA evaluated by reverse transcriptase PCR (RT-PCR). Significant reduction in transcripts for β1 integrin was consistent with the loss of the cell surface protein by FACS. A decrease in Par3 transcripts was also observed, but was either more (A) or less pronounced (B) varying per embryo. GAPDH primers were used as control. In addition, and consistent with the microarray data, qRT-PCR data evaluating 4 separate $\beta1^{f/f}$; Cre+ embryos demonstrated an average reduction of β1 integrin of –3.4 fold with a decrease in Par3 ranging from -.03 to –13 fold and an increase in VE-cadherin transcripts from +0.25 to +0.8 fold and no changes in Par6.

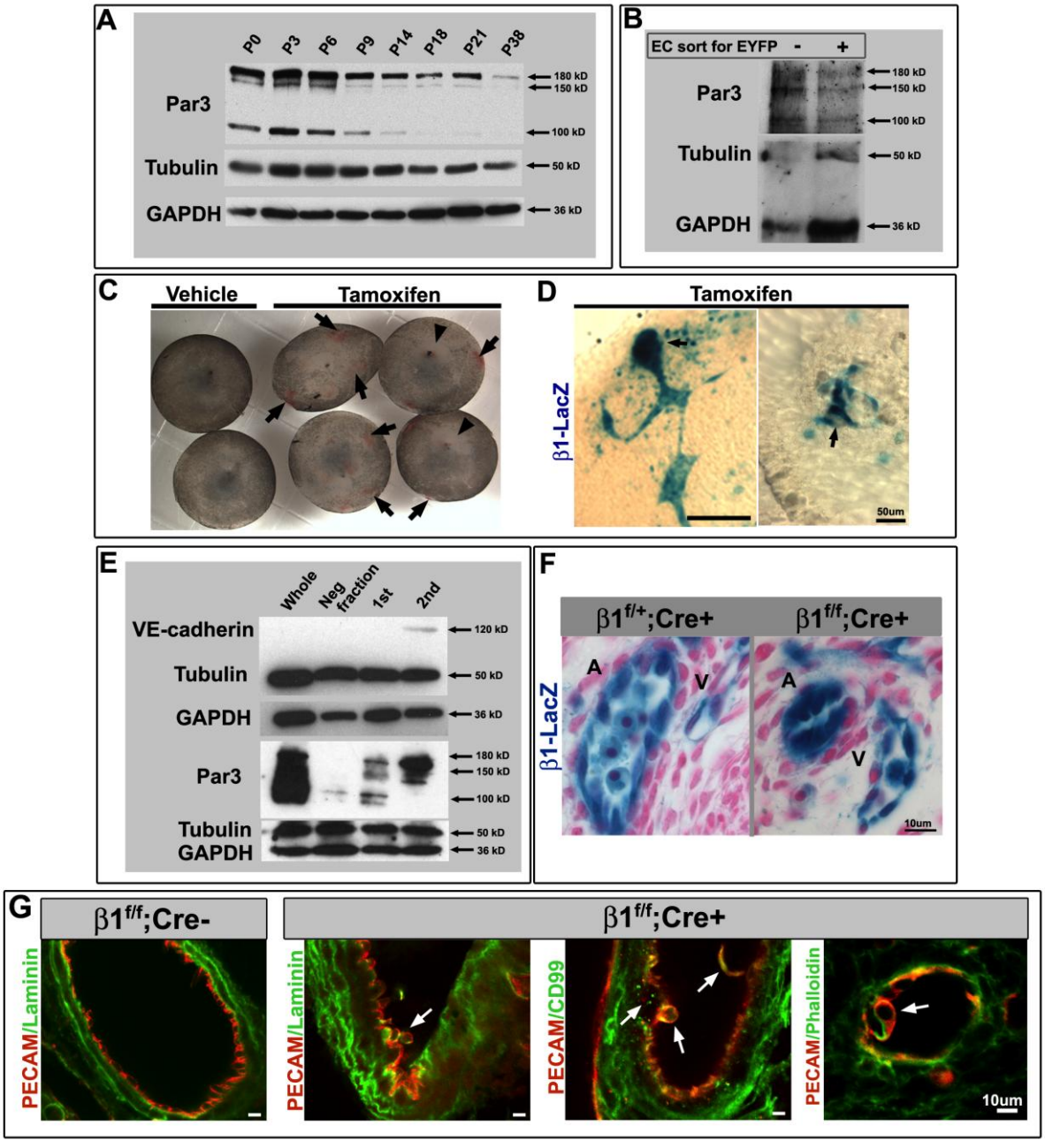

Figure S4: Endothelial specific β1 ablation in the retina and isolation of retinal endothelium. (A) Whole retina cell lysates were evaluated by Western blot for Par3 expression during development, and exhibited an early (P0-P6) expression pattern, in contrast to EC populations (main text, Figure 4A). Tubulin and GAPDH were used as loading controls. (B) Postnatal retinas from P6 to P12 underwent fluorescent activated cell sorting for endothelial cells based on VE-cadherin Cre/R26R EYFP expression. Purified cell populations were combined, and lysates from EYFP+ (endothelial) and

EYFP- (other non-endothelial retinal cells) were evaluated for expression of Par3. Both endothelial and non-endothelial fractions showed expression of Par3 protein. (C) Postnatal ablation of β1 integrin in $\beta1^{f/n}$ transgenic mice results in retinal hemorrhages (arrows) and depigmentation (arrowheads) by P9. (D) Retinal vasculature of the inducible VE-cadherin Cre/$\beta1^{f/n}$ demonstrates cell aggregates and cyst-like formation (arrows). β-gal in blue. (E) Magnetic bead separation of retinal endothelial cells using PECAM-1 demonstrates VE-cadherin protein after the second fractionation, as well as increased Par3 protein levels. (F) β1 integrin promoter is expressed in both arteries (A) and veins (V) within the embryo, as evidenced by β-gal staining (blue), nuclear counterstain in red. (G) Larger embryonic vessels at E15.5 demonstrate cyst-like structures within the endothelial layer (arrows). (D, F, G) Scale bars as labeled per row.

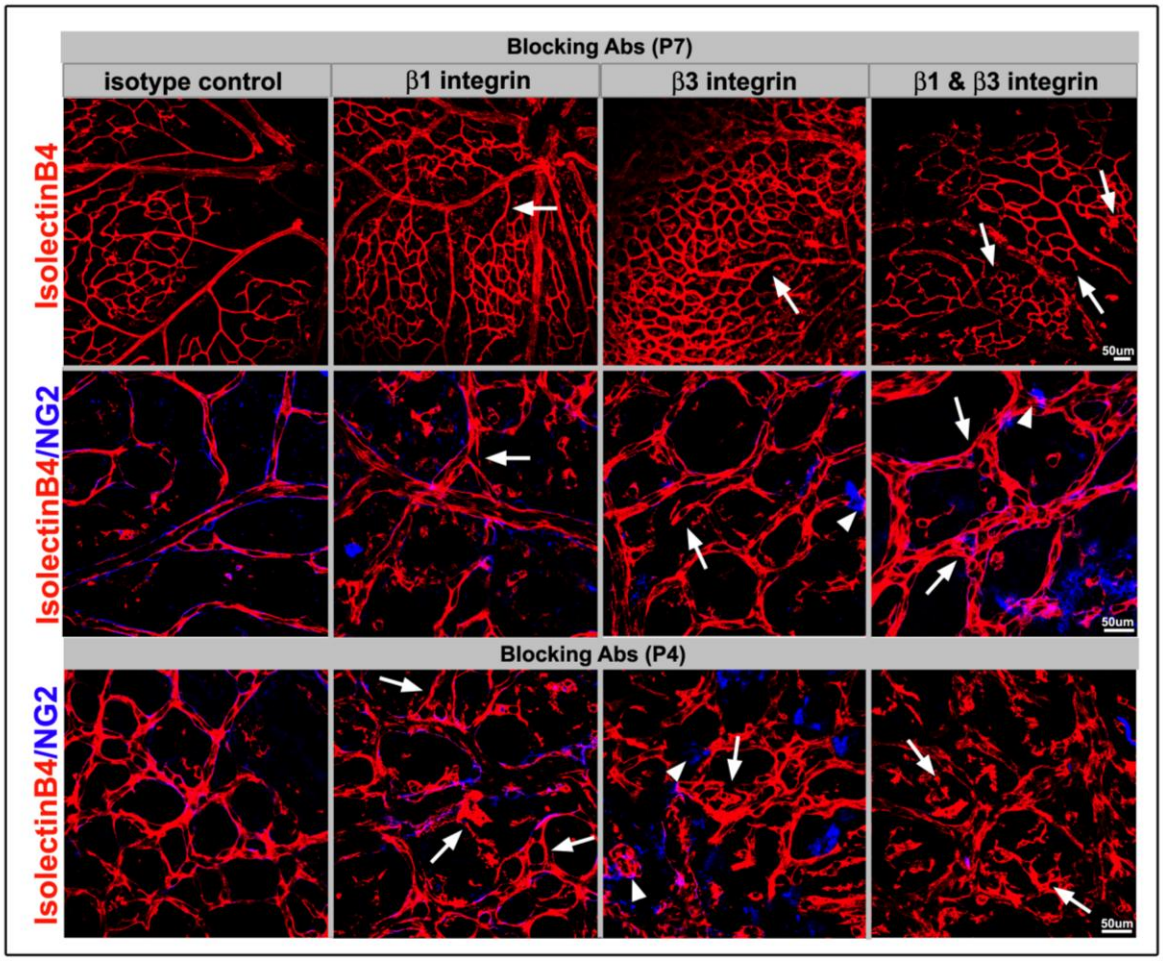

Figure S5: Pharmacological blockade of postnatal retinas (at P7 or P4, evaluated 72hrs later) demonstrate the differences between β1 and β3 ablation (isolectin B4 in red). β1 blockade results in increased branching and abnormal EC localization (arrows), but generally normal pericyte coverage (NG2 in blue). β3 blockade demonstrates abnormal vascular remodeling (arrows) and loss of pericyte coverage (arrowheads). When β1 and β3 are ablated in combination, additive phenotypes are noted: abnormal remodeling and increased branching (arrows) with loss of pericyte coverage (arrowheads). (A-B) Scale bars as labeled per row.

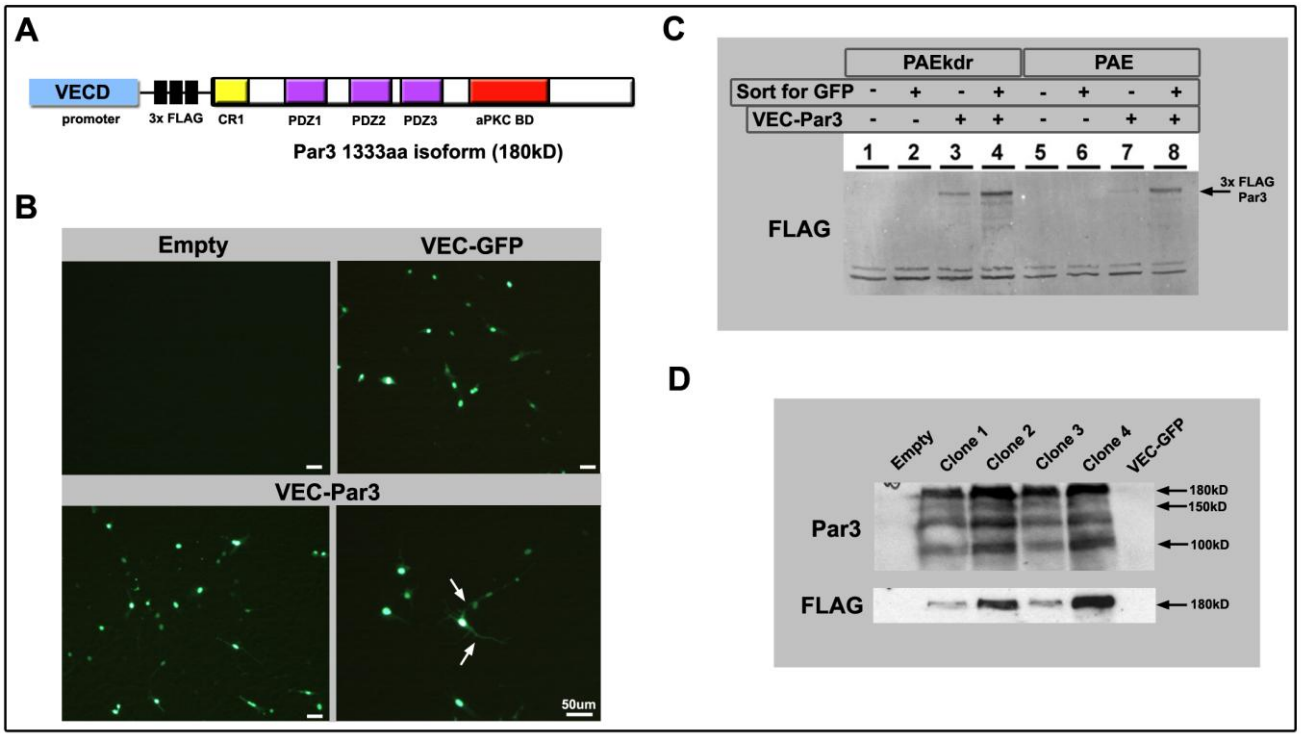

Figure S6: Par3 lentiviral construct. (A) A lentiviral vector was constructed using a VE-Cadherin promoter driving a triple flag tagged Par3 (180 kD isoform). The Par3 180kD isoform contains a dimerization domain (CR1), three PDZ domains and an aPKC binding domain. (B) PAEkdr endothelial cells (porcine aortic endothelial cells with KDR/Flk-1 overexpression) were transfected with plasmids of VEC-GFP (VE-Cadherin driven GFP) and VEC-Par3. Cells transfected with VEC-

Par3 (but not controls) begin to display filopodia like extensions (arrows). Scale bar 50μm for all panels. (C) Two endothelial cell types (PAEkdr and PAE) were infected with VEC-GFP, and a subset with VEC-Par3 (+ or -); when sorted for GFP (+ or -), there was also enrichment for Par3 virally infected cells as detected by anti-FLAG Western blot (~180kD). (D) When separate clones were evaluated for Par3 and FLAG expression, compared to empty vector or GFP alone, each clone exhibited varying levels of Par3 protein (all isoforms) and the FLAG tag.

Supplemental Experimental Procedures

Gene names and nomenclature

In this manuscript Partitioning-Defective Protein 3 is referred to as Par3. The human homolog of this gene is referred to as PAR3 or PARD3 (OMIM 606745). Following SDS-PAGE on 8% PAGE gels and immunoblotting, the most prominent isoform identified in endothelial cell extracts displayed an apparent size of 160-180kD. This size is consistent with the migration of the largest predicted isoform (1333aa variant 3; (NM_033620, GeneID:93742, MGI:2135608). This isoform is predicted to be 149kD in size, yet is reported to run as high as 180kD due to various post translational modifications (Traweger et al., 2008). The predicted molecular weight of FLAG tagged isoform 3 is 152.7kD. When expressed in endothelial cells, the proteins migrated at 180kD, as previously reported for this isoform (Traweger et al., 2008).

Genotyping

Genomic DNA was isolated from tail or yolk sacs by proteinase K (Sigma) digestion and phenol:choroform:isoamyl alcohol extraction. The genotypes were determined by PCR amplification of 100ng of genomic DNA using the following specific primers: for β1 integrin (large construct) lox P1, 5'-AGGTGCCCTTCCCTCTAGA-3'; P2, 5' GTGAAGTAGGTGAAA GGTAAC-3' (PCR

products of 300 bp corresponding to wild type allele and 450bp to loxP allele), β1 integrin (E3 construct) lox F 5'-CGCAGAACAATAGGTGCTGAAATTAC-3' and lox R 5'-GCTACACTGAGAACCACAAACGGC-3' (PCR products of 150 bp corresponding to wild type allele and 190bp to loxP allele), and for Cre recombinase A, 5'-GAACCTGATGGACATGTTCAGGGA-3'; B, 5'-CAGAGTCATCCTTAGCGCCGTAAA-3' (the Cre primers yield a single PCR product of ~971 bp), null allele F 5'-TCACCTCCTAACCCTGAGAT -3' and R 5'-GCAATCCATCTTGTTCAATG-3' (PCR products of 650 bp corresponding to null allele).

RT-PCR and Real-time Analysis

RNA was extracted from $\beta1^{f/f}$; Cre+ endothelial cells, sorted by β1 integrin protein expression, and analyzed as previously described (Lee et al., 2007). GAPDH and β–actin primers were used for internal standards, also as described (Lee et al., 2007). Standard curves for each experimental cDNA were generated by TOPO cloning using standard cloning techniques (Invitrogen). Primers sequences VE-cadherin F 5'-ACGGACAAGATCAGCTCCTC-3' and R 5'-TCTCTTCATCGATGTGCATT-3' (product pair 200bp) (Hudry-Clergeon et al., 2005), β1 integrin F 5'- AATGTTTCAGTGCAGAGC and R 5'-TTGGGATGATGTCGGGAC-3' (product pair 260bp) (Anderson et al., 1999), Par3 F 5'-CCCATGATGACGTGGGATTC-3' and R 5'-GAGAACCGGATCAACATCT-3' (product pair 107) (Fujita et al., 2007), Par6 F 5'- TTCATAAGTCTCAGACCCTAC- 3' and R 5'-GACGCCGACGCAGACCGTCAT-3' (product pair 375bp) (Vinot et al., 2004).

Western blots and endothelial enrichment

Isolated mouse retinas at indicated ages were placed in lysis buffer (1% Triton-X100, 10mM TRIS pH 7.7, 2mM EDTA, 150mM NaCl, 30mM PPiNA, 50mM NaF, 2.1mM Na_3VO_4, 20ng/μl

aprotinin, 10ng/μl leupeptin, and 1mM PMSF), quickly ground with a pestle, then immediately placed into -80 ºC. After one freeze-thaw cycle to lyse the cells, samples were then spun 14,000 rpm at 4 ºC for 30 min. The supernatant was collected and the protein concentration was determined.

For whole retina lysates, 15μg of total protein was loaded onto an 8% acrylamide gel and probed with Par3 (Upstate Biotechnology) at 1:1,000 & 1:5,000, Tubulin (Sigma) at 1:10,000 & 1:20,000, and GAPDH (Chemicon) at 1:5,000 & 1:10,000.

For PECAM-enriched endothelial cell lysates, 30μg of total protein was loaded onto an 8% acrylamide gel and probed with the same above antibodies, but at different concentrations: Par3 at 1:500 & 1:2000, Cre-recombinase 1:500 (Abcam), β1 integrin (Chemicon) at 1:5000 & 1:5000, Tubulin at 1:5000 & 1:5000, α-enolase 1:5000 & 1:10000, and GAPDH at 1:3000 & 1:5000.

Sorted cells were placed in laemmli buffer (with betamercaptoethanol BME) and loaded in equal amounts (200,000 cells) per sample in 8% gels as above. Artery versus vein ECs were harvested by flushing freshly dissected wild-type aorta and inferior vena cava (at the aforementioned ages) with laemmli buffer (+BME) using 0.5ml insulin syringe, loaded in equal amounts and underwent Western blotting as above. Human primary cell lines (passage 4-6) were cultured to confluency, then placed in lysis buffer and processed as above.

In addition a VE-cadherin Cre R26R EYFP line was employed to sort EYFP positive and negative cells in the postnatal retina from P6 to P11 and then quantify Par3 through western blot. Retinas were manually dissociated by pipeting and filtered through 40μm filters and sorted for EYFP expression and 7AAD (BD Pharmingen) for viability.

Isolation of Retinal Endothelium by Immunobeads

Briefly, retinas were dissected, cut into small fragments and subjected to collagenase digestion (0.1mg/ml collagenase, Sigma) for 30min at 37˚C and under agitation. Digested tissue was

further disrupted by pipetting up and down multiple times, the suspension was filtered at 70μm, washed with DMEM through cycles of centrifugation and resuspension and filtered again on a 50μm filter. Cells were then incubated with anti-PECAM antibodies (BD Pharmingen) for 30 min at room temperature followed by incubation with magnetic beads coated with anti-rat secondary antibodies (Invitrogen). Two rounds of magnetic purification were performed per isolation. Twelve to twenty six retinas were used per round of purification to gain a sufficient yield for biochemical analysis. Purity of endothelial isolation was verified by Western blots using VE-cadherin and PECAM antibodies.

Immunohistochemistry

Antigen retrieval and incubation as described in experimental procedures, goat anti-mouse podocalyxin 1:100 (R&D systems), DAPI 1:1000 (Invitrogen).

Supplemental References

Anderson, R., Fassler, R., Georges-Labouesse, E., Hynes, R.O., Bader, B.L., Kreidberg, J.A., Schaible, K., Heasman, J., and Wylie, C. (1999). Mouse primordial germ cells lacking beta1 integrins enter the germline but fail to migrate normally to the gonads. Development (Cambridge, England) *126*, 1655-1664.

Brakebusch, C., Grose, R., Quondamatteo, F., Ramirez, A., Jorcano, J.L., Pirro, A., Svensson, M., Herken, R., Sasaki, T., Timpl, R., *et al.* (2000). Skin and hair follicle integrity is crucially dependent on beta 1 integrin expression on keratinocytes. The EMBO journal *19*, 3990-4003.

Fassler, R., and Meyer, M. (1995). Consequences of lack of beta 1 integrin gene expression in mice. Genes & development *9*, 1896-1908.

Fujita, E., Tanabe, Y., Hirose, T., Aurrand-Lions, M., Kasahara, T., Imhof, B.A., Ohno, S., and Momoi, T. (2007). Loss of partitioning-defective-3/isotype-specific interacting protein (par-3/ASIP) in the elongating spermatid of RA175 (IGSF4A/SynCAM)-deficient mice. The American journal of pathology *171*, 1800-1810.

Hudry-Clergeon, H., Stengel, D., Ninio, E., and Vilgrain, I. (2005). Platelet-activating factor increases VE-cadherin tyrosine phosphorylation in mouse endothelial cells and its association with the PtdIns3'-kinase. Faseb J *19*, 512-520.

Lee, S., Chen, T.T., Barber, C.L., Jordan, M.C., Murdock, J., Desai, S., Ferrara, N., Nagy, A., Roos, K.P., and Iruela-Arispe, M.L. (2007). Autocrine VEGF signaling is required for vascular homeostasis. Cell *130*, 691-703.

Potocnik, A.J., Brakebusch, C., and Fassler, R. (2000). Fetal and adult hematopoietic stem cells require beta1 integrin function for colonizing fetal liver, spleen, and bone marrow. Immunity *12*, 653-663.

Raghavan, S., Bauer, C., Mundschau, G., Li, Q., and Fuchs, E. (2000). Conditional ablation of beta1 integrin in skin. Severe defects in epidermal proliferation, basement membrane formation, and hair follicle invagination. The Journal of cell biology *150*, 1149-1160.
Traweger, A., Wiggin, G., Taylor, L., Tate, S.A., Metalnikov, P., and Pawson, T. (2008). Protein phosphatase 1 regulates the phosphorylation state of the polarity scaffold Par-3. Proceedings of the National Academy of Sciences of the United States of America *105*, 10402-10407.
Vinot, S., Le, T., Maro, B., and Louvet-Vallee, S. (2004). Two PAR6 proteins become asymmetrically localized during establishment of polarity in mouse oocytes. Curr Biol *14*, 520-525.